Microwave measurements of d-f-g-h intervals and d and f fine structure of sodium Rydberg states

X. Sun and K. B. MacAdam
Department of Physics and Astronomy, University of Kentucky, Lexington, Kentucky 40506-0055
(Received 20 September 1993)

Eighty-one microwave resonances in Na Rydberg states $n=21-35$ between d, f, g, and h states have been accurately measured. Among them 43 transitions are first-time measurements, and 38 transitions have been improved, primarily by the elimination of stray electric and magnetic fields, compared with previous measurements. For the d-f transitions, the measured intervals and d-state fine-structure splittings are a factor of 10 more precise; for d-g and d-h series, the measured intervals are a factor of 3 more precise than before. The nf-state fine-structure splittings in Na for $n=21-29$ have also been accurately measured, and the conclusion that the Na f-state fine-structure splitting $nf_{5/2}$-$nf_{7/5}$ is about 5% smaller than the hydrogen f-state fine-structure interval is confirmed through $n=29$.

PACS number(s): 32.30.Bv, 32.80.Rm, 32.60.+i, 35.80.+s

I. INTRODUCTION

In a previous publication [1] we reported 39 microwave transitions in Na Rydberg states $n=22-30$ between d, f, g, and h states. We presented an analysis of the effective dipole and quadrupole core polarizabilities in Na^+ by using the 39 transition frequencies combined with previously measured frequencies [2,3] in the same Rydberg series, $n=9-17$. The average stray electric field in the interaction region was 21 ± 12 mV/cm during the previous measurements [1]. This residual electric field set the maximum of $n=30$ for d-f transitions and $n=28$ for the d-g and d-h transition measurements and limited the accuracy with which line centers could be determined.

A major challenge to precision spectroscopy in Rydberg states is their sensitivity to electric fields, which results from the large geometrical size of the Rydberg atom and the close spacing of adjacent energy levels, particularly in the high-l states. In our recent study [4] of l change induced by ion impact on Na(nd) atoms in Rydberg states, we worked extensively at reducing stray electric fields. The techniques developed in this study, such as constantly heating the plates, using soot-covered plates, providing three-dimensional electric-field bias, and using microwave resonance to detect and correct the stray fields, have been very successful. By using these techniques we were able to limit stray electric fields to about 8 mV/cm. This low stray-field limit allowed us to conduct an extensive series of microwave measurements of Na $\Delta n=0$ d-f, d-g, and d-h transitions by single-photon and multiphoton resonance at frequencies 2–9 GHz for $n=21-35$. For the d-f series the upper limit $n=35$ in this work is set by the lowest microwave frequency (2 GHz) of our Hewlett-Packard Model 8673E oscillator (the energy-level separation of $35d$-$35f$ is about 2.036 GHz). In the case of nd-ng and nd-nh transitions, limitations on the available microwave and radiofrequency (rf) power, the machine-dependent cavity effect, rf Stark shifts, and the existence of the small inhomogeneous stray fields in the interaction region prevented measurement of d-g beyond $n=33$ and d-h beyond $n=32$. We have obtained linewidths narrower than 0.4 MHz for many cases, some as low as 0.2 MHz. We report 81 level separations, and among them 43 are intervals that have not been measured before. We also report nine d-state fine-structure splittings and nine measurements of f-state fine-structure splittings for $n=21-29$.

The experimental method is described in Sec. II. In Sec. III we present the new spectroscopy measurements. In Sec. IV we discuss series-fitting formulas for these transitions, correct the small Stark shifts in the new measurements, and estimate the stray electric fields in the interaction region. In Sec. V we compare the observed nf state fine-structure intervals for sodium to calculated hydrogenic intervals for $n=21-29$. We also compare the observed nd state fine-structure intervals for $n=21-29$ with the best previous values [5].

II. EXPERIMENTAL METHOD

The $\Delta n=0$ electric-dipole single- and multiple-photon transitions are driven by weak applied microwave fields in the same volume of a few mm^3 where Na(nd) Rydberg states are excited from an atomic beam by stepwise pulsed-laser excitation. The transitions are detected by time-resolved selective field ionization (SFI) in the same region. Laser and microwave field pulses are followed after a few μs by an electric-field ramp that field-ionizes the Rydberg atoms, sweeping Na^+ ions into an electron multiplier located outside an assembly of parallel plates. Since the experimental apparatus and procedures were described in detail in previous publications [1,4], we only describe the basic features and explain the modifications made for these experiments. Figure 1 shows the interaction region of the apparatus.

A. Stray magnetic and electric fields

The quadratic Stark effect in inhomogeneous stray electric fields gives asymmetric broadening of the resonance lines on the lower-frequency side and downshifts the resonance peaks. Stray electric fields strongly depend

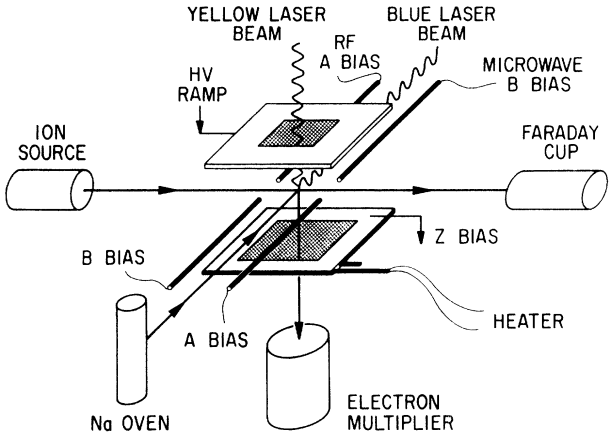

FIG. 1. Schematic diagram of the interaction region of the apparatus.

on the nature of surfaces that surround the interaction region. Five improvements [4] were implemented to reduce stray electric fields in these measurements as compared with the previous measurements [1]. They are (1) SFI plates were uniformly covered by carbon soot, which prevented the plates from charging under the influence of ions; (2) three-dimensional field bias was applied, which significantly reduced the inhomogeneous stray electric fields in the center of the interaction region; (3) the plate assembly was continuously heated to about 120 °C for degassing; (4) the old plates having grid-covered openings were replaced by solid drilled stainless-steel plates to avoid inhomogeneous electric fields caused by contact potential differences between plate and grid materials; (5) a low-density atomic beam (about 10^6 cm^{-3}) was used to avoid collision broadening. With these improvements, the size of the stray electric fields in the interaction region could be reduced to about 8 mV/cm. Lower stray fields could possibly have been attained by taking additional measures if the apparatus were not simultaneously being used for the study of ion-Rydberg collisions [4].

Stray magnetic fields were reduced by Helmholtz coils to about 30 mG in this work by methods described in [1]. The magnetic-field cancellation seemed to be a "one-time" job as long as there were no significant changes in the surroundings, but the stray electric fields changed randomly from time to time, perhaps due to atoms and molecules deposited on the surfaces surrounding the interaction region. The changes were very small and very slow, but failure to detect and correct these changes as they accumulate could cause a downward Stark shift as much as 2 MHz for a $28d$-$28f$ resonance.

B. Microwave resonance

Following laser excitation to *nd* states in the presence of the weak oscillating microwave fields, transitions to *nf*, *ng*, or *nh* occurred during a 3- or 4-μs microwave exposure time. The interaction time of atoms with the microwave radiation could be varied under computer control. The fall time of the microwave pulse was about 40 ns. The SFI ramp was initiated 1 μs after the microwaves were sharply turned off to avoid quantum interference between Stark levels that could occur during the onset of the rising SFI electric field [6]. The frequency scan was carried out automatically under computer control through an IEEE-488 interface.

The *d*-*f* transitions are single-photon electric-dipole transitions that require use of the microwave oscillator at 2–9 GHz. The calculated radiative lifetimes of Na *nd* Rydberg states are long, from 9 to 42 μs for $n=21-35$ [7], and the electric-dipole matrix elements between neighboring states are large, of order $3n(n^2-l^2)^{1/2}a_0/2$ [8], where a_0 is the Bohr radius. For $n \gg l$, matrix elements are of the order of $n^2 a_0$. Therefore a low level of microwave power can drive the *d*-*f* transitions quite easily in a time short compared to the lifetime. In *nd*-*nf* measurements for $n=21-35$, for most of the n values the microwave powers required were only 0.3–2.0 μW (ignoring losses in the crude microwave coupling circuit). But there were some exceptional cases: for $n=21$ it required 20 mW incident microwave power, and for $n=30$ and 33 it only required 0.04 μW microwave power, which is only about 10^{-5} of that required for the $21d$-$21f$ transitions. Theoretically the optimum microwave power required to drive the *d*-*f* transitions in a fixed microwave exposure time can be found from the matrix elements of the electric-dipole operator and is proportional to n^{-4} according to MacAdam and Wing [9]. In free space and under perfect experimental conditions, one could then expect that the microwave power required for the $33d$-$33f$ transitions would be one-sixth of that required for the $21d$-$21f$ transitions. Therefore the huge differences of microwave powers required for *nd*-*nf* transitions in $n=21-35$ can be only explained by machine-dependent cavity effects for some microwave frequencies (here effects of transmission line and termination effects are included in the term "cavity effects"). The cavity created by the electric-field plates and the interaction-region chamber can establish at some frequencies a very strong microwave field in the region of the Rydberg atoms, thus requiring only a low power to drive the transitions. For other frequencies, the cavity effect may cause the microwave field to be very weak if the frequency is far from a cavity resonance or the atoms lie near a node, so more power is required to stimulate the transitions.

As an example of a *d*-*f* transition measurement, Fig. 2 shows the microwave frequency scans of $23d$ to $23f$. The three microwave resonances show the gross separations of $23d$ to $23f$, the $23d$-state fine-structure interval, and $23f$-state fine-structure interval. The microwave resonances directly show that the fine-structure interval of the sodium *nd* state is inverted [10].

For *nd*-*ng* and *nd*-*nh* multiple-photon transitions, both microwave and rf excitations are used. The rf frequency (309–950 MHz, obtained from a Hewlett-Packard Model 8656A source) is fixed to avoid varying cavity effects at the lower frequency, while the microwaves are scanned across the narrow multiple-photon resonance. The microwave scan was kept well away from the single-photon resonance of the *d*-*f* transition. The *d*-*g* transitions are driven with one microwave photon and one rf photon, and the *d*-*h* transitions are driven with one microwave

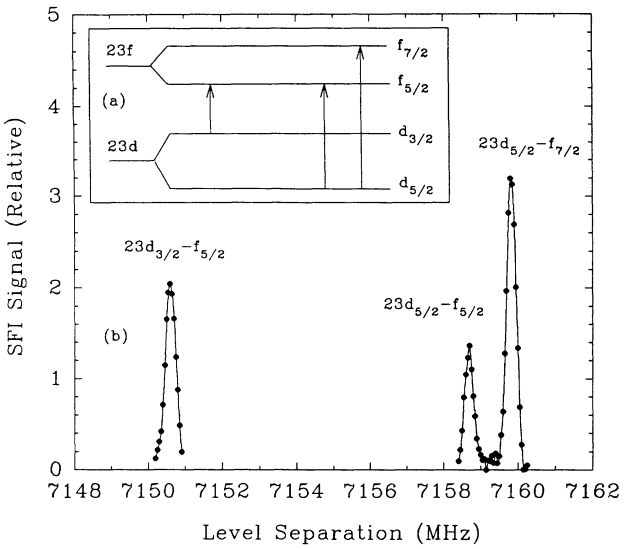

FIG. 2. Na 23*d*-23*f* transitions. (a) Level structure. (b) Microwave resonance scans with nominal microwave power 0.5 mW (13 s per point). The 23*d* state was excited through the Na $3p_{3/2}$ intermediate state.

photon and two rf photons.

The rf field strengths necessary to drive these two- or three-photon transitions easily cause rf or ac Stark shifts [10,11]. Downward shifts as large as several MHz were observed. In order to correct for rf Stark shifts each multiphoton transition was studied at several values of rf power, and the line centers were extrapolated to zero power. Several sets of resonance frequency scans with different rf power for each transition make the extrapolations more accurate. But the cavity effects made some of the multiphoton transitions extremely difficult to measure. For some rf frequencies, there are "dead regions" because of the cavity effect. (Although the apparatus could have been redesigned to avoid these problems, it was intended mainly for another purpose, and redesign was not undertaken.)

The linewidths of *d-g* resonances are noticeably larger than *d-f* linewidths, and the linewidths of *d-h* are much larger than both other series. One possible reason for this is the variations in the rf Stark shift produced by the spatial inhomogeneities of the rf field. As the rf power increases, the resonances exhibit both downshift and asymmetric broadening. Another reason for excess linewidth is the quadratic dc Stark shift. For example, a small stray dc field 10 mV/cm could cause a −0.09-MHz resonance shift for 28*d*-28*f*, −0.39-MHz shift for 28*d*-28*g*, and −1.11 MHz for 28*d*-28*h* according to calculations by Chang [12]. For other n values the Stark coefficients are in corresponding ratios.

III. NEW RESULTS, Na *d-f-g-h* INTERVALS

Eighty-one microwave resonances in Na Rydberg states $n=21-35$ between initial d and final f, g, and h states have been accurately measured in this work, and their frequencies are listed in Tables I and II. (The tabulated resonance frequencies have been extrapolated to zero rf power to correct for rf Stark shifts and have been corrected for dc Stark shifts as described below.) As long as the low-stray-field conditions were maintained, all of these measurements were reproducible within one-third of their linewidths. Typical full widths at half maximum (FWHM) for the *d-f* transitions ranged from 0.2 MHz for the 21*d*-21*f* transition to 0.8 MHz for the 35*d*-35*f* transition exclusive of power broadening. The FWHM of *d-g* transitions ranged from 0.3 MHz for the 22*d*-22*g* transition to 1.4 MHz for the 33*d*-33*g* transition after rf Stark shifts were extrapolated to zero. The *d-h* transitions are most severely affected by inhomogeneous stray fields and by differential rf Stark shifts. They exhibited a FWHM from 1.2 MHz for the 23*d*-23*h* transition to 4 MHz for the 32*d*-32*h* transition.

Attempts to measure higher-l-state transitions such as *nd-ni* were unsuccessful, not only because these higher-order processes required more rf power than was available but also because the higher-l states ($l \geq 6$) are even more sensitive to the stray fields. The estimated 8-mV/cm stray field in the interaction region was big enough to cause the higher states to be so badly broadened as to make the resonances undetectable.

There are two *nd-nf* transition series listed in Tables I and II. Table II lists the *nf*-state fine-structure measurements for $n=21-29$. Since all of these *f*-state fine-structure measurements were conducted within one week without any interruption (e.g., for l-change measurements [4]), and the two series there were measured at least once within each day, the results were very consistent and reproducible during the week of measurements. Values in Table I were made over a longer period of time (about three months), and they accompanied the l-change measurements. They exhibited the larger variations overall as indicated by the standard deviations given in the table. The more accurate measurements for the purpose of extracting a set of *f*-state fine structures are believed to be those in Table II. These are used to obtain the error bars shown in Fig. 4.

IV. SERIES FITTING AND ESTIMATE OF STRAY FIELDS

A. Series fitting

It has been shown empirically [13–15] that level separations *nl-nl'* can be fitted by smooth inverse-power formulas of the type

$$\nu(n)=\sum A^{(M)}n^{-M} . \quad (1)$$

A least-squares program [16] was used to find the values of coefficients $A^{(M)}$ that produce the best fit to a given series of level separations. The standard deviation σ_i for each measured resonance frequency was estimated to be about one-third of its linewidth. Each datum was weighted by σ_i^{-2} in the fitting program. Since the second-order (quadratic) Stark shift increases as n^7 [17], in order to correct for these Stark shifts an additional term $A^{(s)}n^7$ may be added to (1) [1,13]. $A^{(s)}$ is proportional to the square of stray field F,

TABLE I. Level separations (MHz) after Stark corrections. Standard deviation uncertainties, including the uncertainty of Stark corrections, are given in parentheses below each level separation.

n	$d_{3/2}$-$f_{5/2}$	$d_{5/2}$-$f_{7/2}$	$d_{3/2}$-$g_{7/2}$	$d_{5/2}$-$g_{9/2}$	$d_{3/2}$-$h_{9/2}$	$d_{5/2}$-$h_{11/2}$
21	9385.97	9397.94				
	(0.05)	(0.03)				
22	8167.36	8177.79	8900.15			
	(0.05)	(0.03)	(0.20)			
23	7150.73	7159.87	7792.51	7801.18	7941.28	7950.60
	(0.06)	(0.04)	(0.25)	(0.20)	(0.50)	(0.59)
24	6295.95	6304.00	6861.18	6868.80	6992.19	7000.43
	(0.07)	(0.04)	(0.17)	(0.18)	(0.60)	(1.21)
25	5572.06	5579.19	6072.45	6079.19	6188.41	6195.73
	(0.07)	(0.05)	(0.26)	(0.24)	(0.80)	(0.90)
26	4954.96	4961.30	5400.05	5406.05	5503.19	5509.71
	(0.07)	(0.04)	(0.35)	(0.36)	(0.95)	(0.90)
27	4425.67	4431.33	4823.32	4828.67	4915.45	4921.30
	(0.07)	(0.04)	(0.37)	(0.27)	(1.00)	(0.97)
28	3969.12	3974.20	4325.84	4330.63	4408.47	4413.73
	(0.07)	(0.05)	(0.40)	(0.40)	(1.20)	(1.00)
29	3573.24	3577.81	3894.45	3898.77	3968.85	3973.59
	(0.07)	(0.06)	(0.61)	(0.62)	(1.20)	(0.94)
30	3228.27	3232.41	3518.55	3522.44	3585.77	3590.06
	(0.08)	(0.07)	(0.56)	(0.50)	(1.20)	(1.11)
31	2926.30	2930.05	3189.48	3193.01	3250.42	3254.32
	(0.09)	(0.08)	(0.55)	(0.57)	(1.42)	(1.12)
32	2660.83	2664.25	2900.19	2903.40	2955.61	
	(0.10)	(0.08)	(0.75)	(0.65)	(1.50)	
33	2426.52	2429.63	2644.84	2647.77		
	(0.12)	(0.10)	(0.80)	(0.70)		
34	2218.92	2221.76				
	(0.12)	(0.13)				
35	2034.33	2036.94				
	(0.13)	(0.13)				

$$A^{(s)}n^7 = C(l,l')F^2n^7 \ . \tag{2}$$

$C(l,l')n^7$ is an estimate of the average quadratic Stark coefficient for components of the nlj-$nl'j'$ resonance. By use of (1) and (2) the Stark shifts can be estimated from measured transition frequencies, and the stray electric fields can be estimated from the estimated Stark shift and the computed matrix elements for any transition among these measurements. An assumption that a single value of the stray electric field applies to all the fitted measurements underlies the fitting model, and such a field represents therefore a typical, if not actual, value that corresponds to the measuring conditions.

There are several suitable trial models for this series fitting, such as (3,5,7,7'), (3,4,5,7'), and (3,5,7'). [Models based on (1) will be referred to by the set of M exponents selected. "7'" represents the Stark-shift correction term, Eq. (2)].

In the d-f transition series fitting, the most successful fits were obtained with (3,4,5,7') models. But in fitting the four d-g and d-h series, only the (3,5,7') models gave acceptable results in fitting. The reasons for this are ap-

TABLE II. Na Rydberg f-state fine-structure splittings for $n=21$–29. Splittings are obtained by the subtraction of level separations in columns 2 and 3. Level separations are based on new microwave-resonance measurements and are corrected for residual dc Stark shifts. Their standard deviations are obtained from the scatter of repeated measurements (see the text) and are shown as values in the last decimal place by the figures in parentheses. Standard deviations in column 4 are obtained from them in quadrature.

n	$d_{5/2}$-$f_{5/2}$ frequency (MHz)	$d_{5/2}$-$f_{7/2}$ frequency (MHz)	$f_{5/2}$-$f_{7/2}$ interval (MHz)
21	9396.45(1)	9397.94(3)	1.49(3)
22	8176.48(2)	8177.78(1)	1.30(2)
23	7158.73(2)	7159.86(2)	1.13(3)
24	6302.99(2)	6303.99(2)	1.00(3)
25	5578.30(3)	5579.18(3)	0.88(4)
26	4960.51(2)	4961.30(2)	0.79(3)
27	4430.63(2)	4431.33(3)	0.70(4)
28	3973.57(2)	3974.20(3)	0.63(4)
29	3577.24(3)	3577.81(3)	0.57(4)

parently of an experimental origin and not of a fundamental physical significance. The *d-g* and *d-h* transitions are more sensitive to stray electric fields, rf Stark shifts, and cavity effects than *d-f* transitions and are thus expected to be of poorer quality.

B. Estimation of the stray field

We have no direct way to measure the stray electric fields, but the series fitting [1] provided an indirect estimate. If we compare the three types of transitions, i.e., *nd-nf* one-photon transition, *nd-ng* two-photon transitions, and *nd-nh* three-photon transitions, using the three *nd-nf* resonance series fittings alone to estimate the stray fields should be more accurate than using all seven series fittings. One reason for this is the absence of a detectable rf Stark shift in the measurements of *d-f* resonances. Even though the rf Stark shifts were extrapolated to zero in *nd-ng* and *nd-nh* resonance measurements, errors can still be present because of the need to extrapolate. Additionally, the machine-dependent rf cavity effects are most severe for measurements of two-photon and three-photon transitions rendering some transitions unmeasurable. Errors from these two sources having nothing to do with the static stray electric field but increase the errors in the estimation of the stray field by correlations. For these reasons only *d-f* series-fitting results are used here to estimate the stray field.

The (3,4,5,7′) model successfully fitting the three *d-f* resonance series. Stark shifts were negative. The Stark-shift corrections for the three allowed transitions among the four fine-structure levels of the $28d$ state and the $28f$ state were 0.079, 0.063, and 0.034 MHz, corresponding to $28d_{3/2}$-$28f_{5/2}$, $28d_{5/2}$-$28f_{5/2}$, and $28d_{5/2}$-$28f_{7/2}$ transitions, respectively.

Chang and Schoenfeld [12] have calculated the quadratic Stark coefficients of Na $l \geq 2$ levels from perturbation theory. The Stark shift can be expressed as $C(l)n^7F^2$ in a stray electric field F, where $C(l)$ is the Stark-shift coefficient of orbital-angular-momentum state l and n is the principal quantum number. For $n \gg l$,

$$C(l)=8.709\times10^{-11}\ \text{MHz}\,(\text{V/cm})^{-2} \times(l-1/2)l(l+1)(l+3/2)(2l+1)/\alpha_d' \ , \quad (3)$$

where $\alpha_d'=0.9980$ a.u. [1] is the effective dipole polarizability of Na^+. Chang's results for the quadratic Stark-shift coefficients of the Rydberg state Na($28l$) in a stray electric field F in terms of $C(l)(28)^7$ are 185, 1110, 4070, and 11340 MHz $(\text{V/cm})^{-2}$, corresponding to $l=2$, 3, 4, and 5, respectively. By using the quadratic Stark-shift coefficient of $28d$-$28f$ transitions, which is $[C(2)-C(3)](28)^7=-925$ MHz $(\text{V/cm})^{-2}$, and the corresponding three transition resonance Stark-shift corrections from *d-f* series fittings, the stray electric field F was found to be 9.2, 8.3, and 6.1 mV/cm, respectively. So the average stray electric field is estimated to be

$$F=7.9\pm1.3\ \text{mV/cm} \quad (4)$$

in these measurements.

From day to day, the stray-field magnitude apparently varied from 5 to 15 mV/cm. After Stark-shift correction, the resonance of $28d_{5/2}$-$28f_{7/2}$ appears at 3974.20 MHz, which will be regarded as the field-free resonance. Subsequently one could always estimate the magnitude of the stray field in the interaction region by measuring the resonance of this transition alone.

V. THE *d*- AND *f*-STATE FINE-STRUCTURE SPLITTINGS

Tran *et al.* [3] reported previously that the Na *f*-state fine-structure splitting $nf_{5/2}$-$nf_{7/2}$ ($n=9-14$) was about 5% smaller than the hydrogenic value $\alpha^2/2n^3l(l+1)$ a.u., where α is the fine-structure constant. Table II shows new *nf*-state fine-structure splittings measured for $n=21-29$. The fine-structure splittings in this table are obtained by the subtraction of columns 2 and 3. The tabulated resonance frequencies have been corrected for dc Stark shifts by using the (3,4,5,7′) model series fitting, so the fine-structure splittings are automatically corrected for Stark shifts. Typical frequency scans in *f*-state fine-structure interval measurements are shown in Fig. 3.

Table III shows the comparison of *nf* state fine-structure intervals between sodium and calculated hydro-

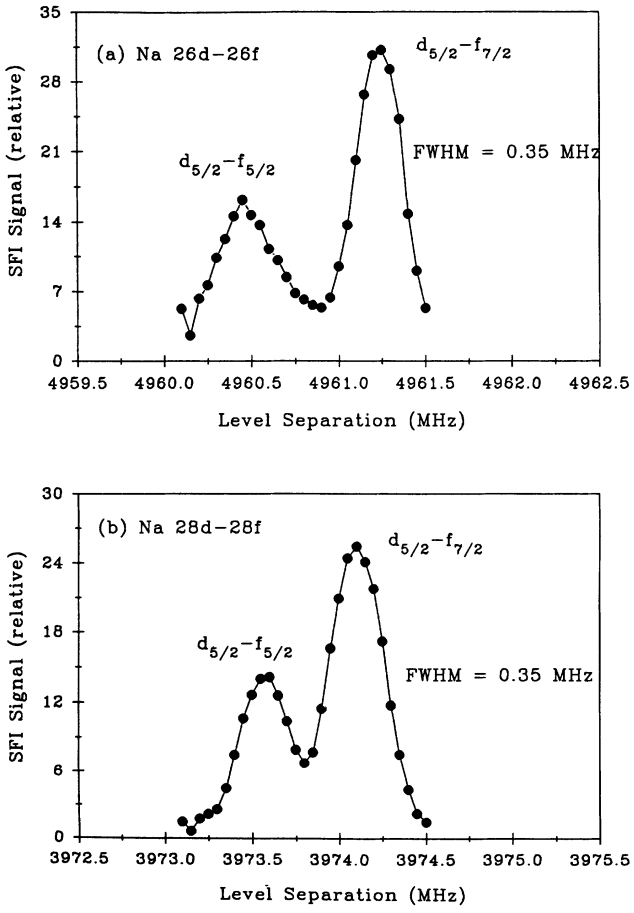

FIG. 3. Frequency scans (0.05-MHz step) of (a) $26d$-$26f$, and (b) $28d$-$28f$, used in measuring *f*-state fine-structure intervals.

TABLE III. Comparison of Rydberg f-state fine-structure splittings of sodium and hydrogen for $n=21-29$. The Na nf-state fine-structure splittings are the same as in Table II.

n	Na f fs interval (MHz)	H fs interval (MHz)	Difference (MHz)	(%)
21	1.49	1.57	−0.08	−5.1
22	1.30	1.37	−0.07	−4.4
23	1.13	1.20	−0.07	−5.0
24	1.00	1.06	−0.06	−4.7
25	0.88	0.93	−0.05	−4.3
26	0.79	0.83	−0.04	−4.8
27	0.70	0.74	−0.04	−5.4
28	0.63	0.66	−0.03	−4.5
29	0.57	0.60	−0.03	−5.0

genic values for $n=21-29$. The average percentage difference of the measured Na f-state fine-structure splittings is 5.2±0.5 % less than hydrogen, and the "5% smaller than hydrogenic" conclusion of Tran *et al.* [3] is confirmed through $n=29$. From the scatter of the percentage differences, the estimated random errors remaining after the Stark-shift correction are about 0.5% of hydrogenic, i.e., 13 kHz at $n=28$, or about (FWHM)/35. The Stark correction for $28f$ was about 0.12 MHz, so the remaining noise is about 10% of the Stark correction.

The ratio of Na nf-state fine-structure intervals (this work, $n=21-29$, and from Tran *et al.* [3], $n=9-14$) to the hydrogen f-state fine-structure intervals are plotted against the principal quantum number n in Fig. 4.

We have also obtained improved values for the nd state fine-structure intervals from $n=21-29$. Table IV shows the d-state fine-structure splittings. Leuchs and Walther [5] have investigated the nd intervals for $n=21-31$, and Jeys *et al.* [18] have measured nd fine structure of selected levels between $n=32$ and 40. Both sets of results, obtained by quantum-beat spectroscopy, are compared with our results in Fig. 5. The values for nd fine-structure intervals are multiplied by n^3 and plotted as a function of n, where a horizontal line would thus indicate a scaling as $1/n^3$. Our measurements are a factor of 10 more precise than the values of Leuchs and Walther. All measurements illustrate the expected scaling, but our measurements are consistently about 2.6% lower than the values of Jeys *et al.* as shown in the figure. The source of this systematic discrepancy might be a proportional error in time per channel of the quantum-beat experiments, but it is difficult to see how an error of this proportional form and magnitude could occur in the microwave resonances.

TABLE IV. Na Rydberg d-state fine-structure splittings for $n=21-29$. Splittings are obtained by subtraction of the level separations in columns 2 and 3. Level separations are based on new microwave-resonance measurements and are corrected for residual dc Stark shifts. Their standard deviations are obtained from the scatter of repeated measurements and are shown as values in the last decimal place by the figures in parentheses. Standard deviations in column 4 are obtained from them in quadrature.

n	$d_{5/2}$-$f_{5/2}$ frequency (MHz)	$d_{3/2}$-$f_{5/2}$ frequency (MHz)	$d_{5/2}$-$d_{3/2}$ interval (MHz)
21	9396.45(1)	9385.97(5)	10.48(5)
22	8176.48(2)	8167.36(5)	9.12(5)
23	7158.73(2)	7150.73(6)	8.00(6)
24	6302.99(2)	6295.95(7)	7.04(7)
25	5578.30(3)	5572.06(7)	6.24(8)
26	4960.51(2)	4954.96(7)	5.55(7)
27	4430.63(2)	4425.67(7)	4.96(7)
28	3973.57(2)	3969.12(7)	4.45(7)
29	3577.24(3)	3573.24(7)	4.00(8)

The microwave-resonance technique is a sensitive probe of stray-field effects [19]. By reducing the stray field to about 8 mV/cm, we have considerably improved the accuracy of our previous measurements and further fulfilled the high-n, d-f-g-h, spectroscopy of Na by adding 43 new resonances. For $n=21-29$, the f-state fine-structure intervals are 4–5 % smaller than in hydrogen. Some discrepancies remain in the measurements of nd fine-structure intervals, $n=21-40$, at the 2–3% level. On the other hand, microwave frequency l splittings are reported here, in several cases, with accuracies better than 10 parts per million.

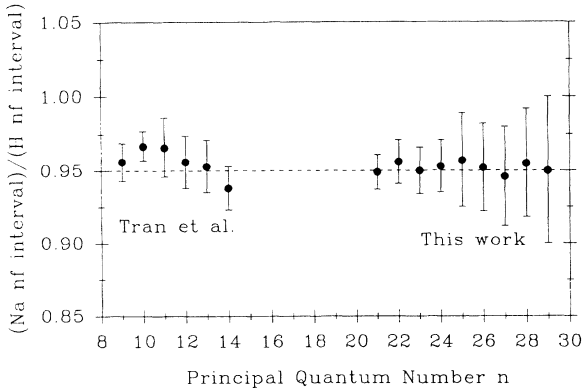

FIG. 4. The ratio of f-state fine-structure intervals for sodium and hydrogen. The dashed line represents a value 0.95. Measurements for $n=9-14$, Ref. [3].

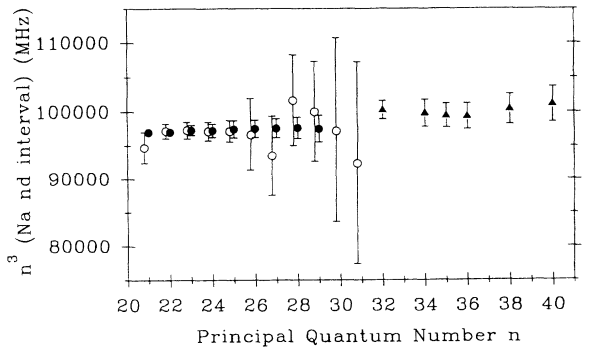

FIG. 5. d-state fine-structure intervals are multiplied by n^3 and plotted as a function of n. Solid dots, this work; open circles, Leuchs and Walther [5] (offset slightly to the left for clarity); triangles, Jeys *et al.* [18].

ACKNOWLEDGMENTS

We acknowledge the assistance and contributions of Dr. Lewis Gray in the course of this work, which was supported by the National Science Foundation through Grant No. PHY-8808022.

[1] L. G. Gray, X. Sun, and K. B. MacAdam, Phys. Rev. A **38**, 4985 (1988).

[2] T. F. Gallagher, R. M. Hill, and S. A. Edelstein, Phys. Rev. A **14**, 744 (1976).

[3] N. H. Tran, H. B. van Linden van den Heuvell, R. Kachru, and T. F. Gallagher, Phys. Rev. A **30**, 2097 (1984).

[4] X. Sun and K. B. MacAdam, Phys. Rev. A **47**, 3913 (1993).

[5] G. Leuchs and H. Walther, Z. Phys. A **293**, 93 (1979).

[6] J. Singh, X. Sun, and K. B. MacAdam, Phys. Rev. Lett. **58**, 2201 (1987).

[7] J. F. Gounand, J. Phys. (Paris) **40**, 457 (1979).

[8] H. A. Bethe and E. A. Salpeter, *Quantum Mechanics of One and Two Electron Atoms* (Academic, New York, 1957).

[9] K. B. MacAdam and W. H. Wing, Phys. Rev. A **12**, 1464 (1975).

[10] T. F. Gallagher, R. M. Hill, and S. A. Edelstein, Phys. Rev. A **13**, 1448 (1976).

[11] S. H. Autler and C. H. Townes, Phys. Rev. **100**, 703 (1955).

[12] E. S. Chang and W. G. Schoenfeld, Astrophys. J. **383**, 450 (1991).

[13] K. B. MacAdam and W. H. Wing, Phys. Rev. A **13**, 2163 (1976).

[14] W. H. Wing and K. B. MacAdam, in *Progress in Atomic Spectroscopy, Part A,* edited by W. Hanle and H. Kleinpoppen (Plenum, New York, 1978), p. 491.

[15] J. W. Farley, K. B. MacAdam, and W. H. Wing, Phys. Rev. A **20**, 1754 (1979).

[16] P. R. Bevington, *Data Reduction and Error Analysis for the Physical Sciences* (McGraw-Hill, New York, 1969), Chap. 6.

[17] J. J. Sakurai, in *Modern Quantum Mechanics,* edited by S. F. Tuan (Benjamin/Cummings, Menlo Park, CA, 1985), p. 296.

[18] T. H. Jeys, K. A. Smith, F. B. Dunning, and R. F. Stebbings, Phys. Rev. A **23**, 3065 (1981).

[19] E. A. Hessels, F. J. Deck, P. W. Arcuni, and S. R. Lundeen, Phys. Rev. A **41**, 3663 (1990); F. J. Deck and S. R. Lundeen, *ibid.* **46**, 2622 (1992).

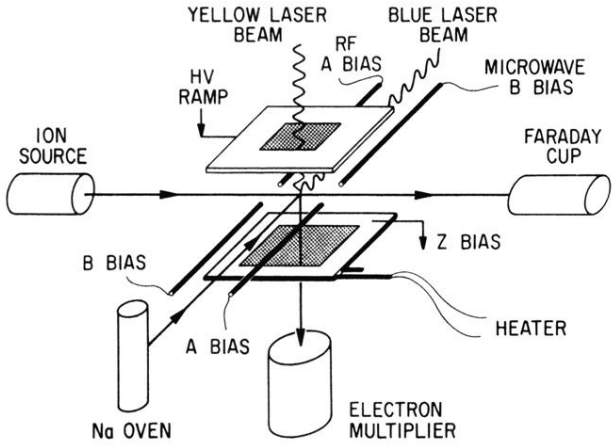

FIG. 1. Schematic diagram of the interaction region of the apparatus.